NIH Public Access
Author Manuscript
Virology. Author manuscript; available in PMC 2008 December 9.

Published in final edited form as:
Virology. 2006 September 30; 353(2): 283–293. doi:10.1016/j.virol.2006.04.042.

Role of Cellular FKBP52 Protein in Intracellular Trafficking of Recombinant Adeno-associated Virus 2 Vectors

Weihong Zhao[a,b], **Li Zhong**[a], **Jianqing Wu**[a,b], **Linyuan Chen**[a], **Keyun Qing**[c], **Kirsten A. Weigel-Kelley**[a], **Steven H. Larsen**[d], **Weinian Shou**[e], **Kenneth H. Warrington Jr.**[a], and **Arun Srivastava**[a*]

a*The Division of Cellular and Molecular Therapy, Departments of Pediatrics, Molecular Genetics & Microbiology, Powell Gene Therapy Center University of Florida College of Medicine, Gainesville, FL 32610, USA*

b*The First Affiliated Hospital of Nanjing Medical University, Nanjing, Jiangsu, 210029 P.R. China*

c*Eli Lilly & Company, Indianapolis, IN 46285, USA*

d*Department of Microbiology & Immunology, Indiana University School of Medicine, Indianapolis, IN 46202, USA*

e*Herman B Wells Center for Pediatric Research and Department of Molecular Biology & Biochemistry, Indiana University School of Medicine, Indianapolis, IN 46202, USA*

Abstract

We have reported that tyrosine-phosphorylated forms of a cellular protein, FKBP52, inhibit the second-strand DNA synthesis of adeno-associated virus 2 (AAV), leading to inefficient transgene expression from recombinant AAV vectors. To further explore the role of FKBP52 in AAV-mediated transduction, we established murine embryo fibroblasts (MEFs) cultures from FKBP52 wild-type (WT), heterozygous (HE), and knockout (KO) mice. Conventional AAV vectors failed to transduce WT MEFs efficiently, and the transduction efficiency was not significantly increased in HE or KO MEFs. AAV vectors failed to traffick efficiently to the nucleus in these cells. Treatment with hydroxyurea (HU) increased the transduction efficiency of conventional AAV vectors by ~25-fold in WT MEFs, but only by ~4-fold in KO MEFs. The use of self-complementary AAV (scAAV) vectors, which bypass the requirement of viral second-strand DNA synthesis, revealed that HU treatment increased the transduction efficiency ~23-fold in WT MEFs, but only ~4-fold in KO MEFs, indicating that the lack of HU treatment-mediated increase in KO MEFs was not due to failure of AAV to undergo viral second-strand DNA synthesis. Following HU treatment, ~59% of AAV genomes were present in the nuclear fraction from WT MEFs, but only ~28% in KO MEFs, indicating that the pathway by which HU treatment mediates nuclear transport of AAV was impaired in KO MEFs. When KO MEFs were stably transfected with an FKBP52 expression plasmid, HU treatment-mediated increase in the transduction efficiency was restored in these cells, which correlated directly with improved intracellular trafficking. Intact AAV particles were also shown to interact with FKBP52 as well as with dynein, a known cellular protein involved in AAV trafficking. These studies

*Corresponding author: Dr. Arun Srivastava, Division of Cellular & Molecular Therapy, Department of Pediatrics, University of Florida College of Medicine, 13706 Innovation Drive, Room 201, Progress Park, Alachua, FL 32615, USA; Fax: 386-462-4099, E-mail address: asrivastava@gtc.ufl.edu.

Publisher's Disclaimer: This is a PDF file of an unedited manuscript that has been accepted for publication. As a service to our customers we are providing this early version of the manuscript. The manuscript will undergo copyediting, typesetting, and review of the resulting proof before it is published in its final citable form. Please note that during the production process errors may be discovered which could affect the content, and all legal disclaimers that apply to the journal pertain.

NIH-PA Author Manuscript
NIH-PA Author Manuscript
NIH-PA Author Manuscript

NIH-PA Author Manuscript

NIH-PA Author Manuscript

NIH-PA Author Manuscript

suggest that FKBP52, being a cellular chaperone protein, facilitates intracellular trafficking of AAV, which has implications in the optimal use of recombinant AAV vectors in human gene therapy.

Keywords

Adeno-associated virus type 2; Viral vectors; Murine embryo fibroblasts; FK506-binding protein; Intracellular trafficking; Gene transfer; Gene expression

Introduction

Adeno-associated virus 2 (AAV), a non-pathogenic human parvovirus, has gained attention as a potentially safe vector for gene transfer and gene therapy (Conlon and Flotte, 2004; Marshall, 2001). The AAV genome is a single-stranded DNA (Berns and Giraud, 1996; Muzyczka, 1992), which is transcriptionally inactive. Others and we have suggested that viral second-strand DNA synthesis is the rate-limiting step in AAV-mediated transgene expression (Ferrari et al., 1996; Fisher et al., 1996; Mah et al., 1998; Qing et al., 2001; Qing et al., 1998; Qing et al., 2003; Qing et al., 1997; Zhong et al., 2004a; Zhong et al., 2004b; Zhong et al., 2004c; Zhong et al., 2004d). In our previous studies, we have identified that a 52-kDa cellular protein, FKBP52, which binds the immunosuppressant drug, FK506, interacts specifically with the D-sequence within the inverted terminal repeat (ITR) of the AAV genome (Qing et al., 2001; Zhong et al., 2004a; Zhong et al., 2004b; Zhong et al., 2004c; Zhong et al., 2004d). FKBP52 is phosphorylated at both tyrosine and serine or threonine residues, and phosphorylated FKBP52 inhibits the viral second-strand DNA synthesis, leading to inefficient transgene expression (Mah et al., 1998; Qing et al., 2001; Qing et al., 1998; Qing et al., 2003; Qing et al., 1997; Zhong et al., 2004a; Zhong et al., 2004b; Zhong et al., 2004c; Zhong et al., 2004d). We have also documented that FKBP52 is dephosphorylated at tyrosine residues by the cellular T cell protein tyrosine phosphatase (TC-PTP), and dephosphorylated FKBP52 can no longer bind to the D-sequence, thereby allowing viral second-strand DNA synthesis and, consequently, efficient transgene expression (Qing et al., 2003; Zhong et al., 2004a; Zhong et al., 2004b; Zhong et al., 2004c; Zhong et al., 2004d).

Our previous studies with FKBP52-knockout (FKBP52-KO) mice, in which FKBP52 is completely absent, documented that the transduction efficiency in hematopoietic stem/progenitor cells and hepatocytes was significantly less pronounced than that from TC-PTP-transgenic (TC-PTP-TG) mice, in which FKBP52 is dephoshorylated at tyrosine residues (Zhong et al., 2004a; Zhong et al., 2004b; Zhong et al., 2004c). We have also reported that AAV vectors transduce an established murine fibroblast cell line poorly due to impaired intracellular trafficking (Hansen et al., 2000; Hansen, Qing, and Srivastava, 2001a), and that deliberate over-expression of FKBP52 significantly increases the transduction efficiency in these cells (Qing et al., 2001). Although we interpreted these data to suggest that over-expression of FKBP52 led to dephosphorylation at tyrosine residues of the endogenous FKBP52 in the nucleus, the precise role of FKBP52 in the cytoplasm remained unclear. This is of significance since FKBP52 has been documented to interact with HSP90 only when in the dephosphorylated form, and this complex has been shown to mediate cytoplasmic transport of a number of cellular and viral proteins to the nucleus (Czar et al., 1994a; Czar et al., 1994b; Denny et al., 2005; Perrot-Applanat et al., 1995; Pratt, 1998; Pratt et al., 2004; Pratt, Silverstein, and Galigniana, 1999; Pratt and Toft, 1997; Wochnik et al., 2005; Wu et al., 2004). FKBP52 is a cellular chaperone protein, and ~80% is localized in the nucleus, and ~20% in cytoplasm, where it co-localizes with microtubules and dynein, a retrograde motor protein, where the PPIase domain fragment of FKBP52 interacts with dynein (Czar et al., 1994a; Czar et al., 1994b; Perrot-Applanat et al., 1995). Thus, in addition to studying the interaction of FKBP52 with the D-sequence in the AAV ITR, and its role in inhibiting viral second-strand

NIH-PA Author Manuscript

NIH-PA Author Manuscript

NIH-PA Author Manuscript

DNA synthesis in the nucleus, we also wished to examine the role of FKBP52 present in the cytoplasm in AAV-mediated transduction. To this end, we generated primary mouse embryo fibroblasts (MEFs) from FKBP52-wild-type (WT), heterozygous (HE), and knockout (KO) mice, and examined various steps in the life cycle of recombinant AAV vectors in these cells under a variety of conditions.

Our studies reported here suggest that in MEFs, AAV vectors fail to gain entry into the nucleus. Treatment with hydroxyurea (HU) promotes AAV nuclear transport, and FKBP52 can facilitate this process. Thus, in addition to interacting with the D-sequence in the AAV ITR, and inhibiting viral second-strand DNA synthesis in the nucleus, FKBP52, being a cellular chaperone protein, may also facilitate intracellular trafficking of AAV, which has implications in the optimal use of recombinant AAV vectors in human gene therapy.

Results

MEFs from WT as well as KO Mice are transduced poorly by AAV vectors, which is not due to compensatory binding of a cellular protein to the AAV D-sequence

Murine embryo fibroblasts (MEFs) from FKBP52 wild-type (WT), heterozygous (HE), and knockout (KO) mice, established following immortalization using wild-type SV40 virus infections, were either mock infected or infected with a recombinant AAV2-*lacZ* vectors under identical conditions. β-galactosidase activity was measured 48 h post-infection. These results are shown in Fig. 1A. As is evident, no transgene expression was detected in mock-infected cells, and the transduction efficiency in WT MEFs was low. Although reduction in the levels of FKBP52 in HE and complete absence in KO MEFs were expected to augment viral second-stranded DNA synthesis, the transduction efficiency of AAV vectors was not significantly increased in HE and KO cells. The lack of transgene expression was not a consequence of immortalization by SV40 virus infection since primary MEFs from these mice were also transduced poorly by AAV vectors (data not shown). We next wished to determine whether compensatory binding of a putative cellular protein to the AAV D-sequence in the absence of FKBP52 in KO MEFs was responsible for impaired viral second- strand DNA synthesis. To this end, electrophoretic mobility shift assays (EMSA) were performed using WCEs prepared from MEFs of each genotype. These results are shown in Fig. 1B. As can be seen, the AAV D-sequence probe (Lane 1) formed a complex only with WCEs from WT (Lane 4), and to ~50% lesser extent in HE MEFs (Lane 3). No complex formation was detected with WCEs from KO MEFs (Lane 2). These data suggested that in the absence of FKBP52, the observed lack of AAV-mediated transgene expression in KO MEFs was not due to the presence of a cellular protein that compensated for binding to the AAV D-sequence leading to impaired viral second-strand DNA synthesis.

The lack of AAV-mediated transgene expression in MEFs is not due to the absence of cellular receptor and co-receptor required for viral binding and entry

Since it remained possible that sub-optimal levels of expression of heparan sulfate proteoglycan (HSPG) and fibroblast growth factor receptor 1 (FGFR1), the cellular receptor and co-receptor, respectively, for AAV (Qing et al., 1999; Summerford, Bartlett, and Samulski, 1999), were responsible for inefficient viral binding and entry into MEFs, we next performed fluorescence-activated cell sorting (FACS) analyses, the results of which are shown in Fig. 2A. It is clear that ~ 41.14%, 46.44% and 49.51% of MEFs from WT, HE and KO mice respectively, expressed HSPG. Approximately 61.74%, 66.54%, and 63.82% of MEFs from WT, HE and KO mice respectively, expressed FGFR1. Although we did not analyze these cells for co-expression of HSPG and FGFR1, we performed Southern blot analyses to detect entry of viral DNA. Briefly, equivalent numbers of each cell type were infected with a recombinant AAV-*lacZ* vector for 2 h at 37°C and treated with trypsin to degrade any adsorbed viral particles.

NIH-PA Author Manuscript

NIH-PA Author Manuscript

NIH-PA Author Manuscript

Low M_r DNA samples were analyzed on Southern blots using a *lacZ*-specific DNA probe. These results are shown in Fig. 2B. The fact that roughly the same level of hybridization to input single-stranded AAV genomes was detected, these data corroborate that AAV could efficiently enter MEFs from each of the three genotypes. Thus, the absence of FKBP52 did not appear to influence viral binding and entry into KO cells.

Hydroxyurea treatment can increase the transduction efficiency of conventional, single-stranded AAV vectors in WT and HE MEFs, but to a lesser extent in KO MEFs

Hydroxyurea (HU) is a chemotherapeutic agent and its mechanism of action is believed to be based on its inhibition of the enzyme ribonucleotide reductase. It has been reported that HU treatment increases AAV-mediated transduction of many cell types by causing S-phase arrest with a concomitant increase in the DNA repair synthesis, which may be crucial for viral second-strand DNA synthesis (Russell, Alexander, and Miller, 1995). However, mechanisms other than inhibition of ribonucleotide reductase might be responsible for increasing AAV-mediated transduction. For example, we have reported that the transduction efficiency of AAV vectors can be significantly augmented in the murine established fibroblast cell line, NIH3T3, and in primary hematopoietic stem/progenitor cells following treatment with HU, because HU facilitates nuclear transport of AAV in these cells (Hansen, Qing, and Srivastava, 2001a; Zhong et al., 2004c) as well as leads to dephosphorylation of FKBP52 at tyrosine residues (Qing et al., 1997; Qing et al., 1998; Mah et al., 1998). We wished to examine whether HU could also increase the transduction efficiency of AAV vectors in MEFs. We reasoned that HU would promote AAV trafficking into the nucleus, and would result in higher transduction efficiency in KO MEFs compared with that than in WT MEFs because the absence of FKBP52 in the former would facilitate viral second-stranded DNA synthesis. Each of the genotype cells were either mock-treated or treated with 10 mM or 40 mM HU for 12 h prior to AAV-mediated transduction, and transgene expression was determined 48 h post-transduction. These results are shown in Fig. 3A It is evident that treatment with HU did increase the AAV transduction efficiency ~15–25-fold, in a dose-dependent manner in WT MEFs, and ~7-fold in HE MEFs. Surprisingly, however, the transduction efficiency in KO MEFs was increased by only ~3–4-fold [$p<0.001$].

Since in our previous studies, we had determined that impaired intracellular trafficking of AAV into the nucleus in the NIH3T3 cell line limits high-efficiency transduction of these cells (Hansen et al., 2000; Hansen, Qing, and Srivastava, 2001a), we reasoned that the lack of significant increase in AAV transduction of KO MEFs might also be due to inefficient transport of AAV from cytosol into the nucleus. To corroborate this, nuclear and cytoplasmic fractions of MEFs were obtained 48 h post-infection. Low M_r DNA was isolated from these fractions and analyzed on Southern blots. These results are shown in Fig. 3B. As can be seen, whereas nearly 100% of the input AAV ssDNA was present in the cytoplasmic fraction in MEFs from all three genotypes (Lanes 2,4,6), treatment with HU promoted nuclear transport of AAV in each MEFs (Lanes 7,9,11). Densitometric analyses of these data, shown in Fig. 3B, revealed that following HU treatment, AAV DNA in the nuclear fraction increased to ~58.5% in WT MEFs, whereas in KO MEFs, the increase was only ~28.1%. These data suggest that in the absence of FKBP52, treatment with HU is not sufficient for the optimal transport of AAV into the nucleus, which also correlates with the lower transduction efficiency in KO MEFs.

HU treatment can also increase the transduction efficiency of double-stranded, self-complementary AAV vectors in WT and HE MEFs, but to a lesser extent in KO MEFs

In addition to promoting AAV intracellular trafficking, HU can also dephosphorylate FKBP52 and increase AAV second-strand DNA synthesis (Hansen, Qing, and Srivastava, 2001a; Hansen, Qing, and Srivastava, 2001b; Qing et al., 1998; Zhong et al., 2004c). In order to determine whether the observed lack of increase in the transduction efficiency of AAV vectors

NIH-PA Author Manuscript

NIH-PA Author Manuscript

NIH-PA Author Manuscript

in KO MEFs following HU treatment was related to viral second-strand DNA synthesis, we utilized double-stranded, self-complementary AAV (scAAV) vectors that obviate the need for viral second-strand DNA synthesis (McCarty, Monahan, and Samulski, 2001; Wang et al., 2003). Transduction efficiency of scAAV-EGFP vectors was evaluated 48 h post-infection in WT, HE, and KO MEFs, with and without prior treatment with 40 mM HU. These results are shown in Fig. 4A. As can be seen, although scAAV vectors bypass the requirement of viral second-strand DNA synthesis, the transduction efficiency of these vectors in MEFs of all the three genotypes was still very low, but could be increased by HU treatment. Quantitative analyses of these data, shown in Fig. 4B, indicated that HU treatment increased scAAV vector transduction efficiency in WT MEFs ~23-fold, but only ~4-fold in KO MEFs [$p < 0.001$]. These data suggest that the observed differential transduction efficiency of AAV vectors in WT and KO MEFs, following HU treatment, is not directly related to viral second-strand DNA synthesis.

Deliberate expression of FKBP52 in KO MEFs restores the normal response to HU-induced increase in AAV transduction efficiency

To further evaluate the role of FKBP52 in AAV-mediated transduction of MEFs, we generated a eukaryotic expression plasmid containing the human FKBP52 gene under the control of the Rous sarcoma virus promoter (pRSV-hFKBP52). Since murine and human FKBP52 share 95% homology (Sanchez et al., 1990; Schmitt, Pohl, and Stunnenberg, 1993), we reasoned that expression of its human counterpart might be functional in KO MEFs. KO cells were stably transfected with this plasmid to generate KO-T cells, and the levels of expression of FKBP52 were detected by Western blot analyses. These data are shown in Fig. 5A. Densitometric scanning of lumigraphs revealed the level of expression of FKBP52 in KO-T cells was between the levels of WT and that of HE MEFs. In the next set of experiments, KO and KO-T MEFs were either mock infected or infected with recombinant AAV-*lacZ* vectors with or without prior treatment with HU, and transgene expression was evaluated 48 h post-infection. These results are shown in Fig. 5B. It is evident that, consistent with our previous data, AAV transduction efficiency was low in KO MEFs (Panel b), and HU treatment had little effect (Panel c). The transduction efficiency was also low in KO-T cells (Panel e), but was significantly increased following HU treatment (Panel f). Nuclear and cytoplasmic fractions of KO and KO-T cells were obtained 48 h post-infection, low M_r DNA was isolated from these fractions and analyzed on Southern blots. These results are shown in Fig. 5C. It is evident that, consistent with our previous data, nearly 100% of the input AAV ssDNA was present in the cytoplasmic fraction in KO (Lane 1) as well as in KO-T (Lane 3) cells, treatment with HU promoted nuclear transport of AAV in both cell types (Lanes 6,8). Densitometric analyses of these data, shown in Fig. 5D, indicated that the input AAV single-stranded DNA in the nuclear fraction increased from ~27.2% in KO cells to ~61.9% in KO-T cells. Thus, FKBP52 is able to restore normal response to HU treatment for AAV-mediated transgene expression in FKBP52-KO MEFs.

Intact AAV capsids associate with FKBP52

We next examined whether FKBP52 also interacts with intact AAV particles to facilitate intracellular trafficking. However, these studies could not be performed in MEFs in view of their low infection as well transfection efficiency, for which 293 cells were used instead. Cells were either mock-transfected or co-transfected with the following three plasmids, recombinant AAV vector (pAAV-hrGFP), an adenovirus helper (pHelper), and an AAV helper (pAAV2-RC) to generate AAV-GFP vectors (12–15,42). Cells were harvested 72 h post-transfection by scraping, and resuspended in a hypotonic buffer. Cytoplasmic fraction was isolated by homogenization in a tight-fitting Duall tissue grinder. Equivalent amounts of cytoplasm were immunoprecipitated with A20 antibodies, which specifically recognize only intact AAV particles with a defined three-dimensional structure (Wistuba et al., 1997; Wobus et al.,

NIH-PA Author Manuscript

NIH-PA Author Manuscript

NIH-PA Author Manuscript

2000), and analyzed on Western blots. Immunoprecipitation with normal goat IgG antibodies was performed as a negative control. These results are shown in Fig. 6. As can be seen, intact AAV capsids associate with FKBP52 as well as dynein, known to interact with FKBP52 (Wochnik et al., 2005). These data document that FKBP52 acts as an accessory protein and may be involved in intracellular trafficking of AAV directly or indirectly through dynein.

Discussion

It is now firmly established that the viral second-stranded DNA synthesis is a major rate-limiting step in AAV-mediated transgene expression, and that a cellular protein, FKBP52, is a negative regulator of this step in the virus life cycle (Ferrari et al., 1996; Fisher et al., 1996; Mah et al., 1998; Qing et al., 2001; Qing et al., 1998; Qing et al., 2003; Qing et al., 1997; Zhong et al., 2004a; Zhong et al., 2004b; Zhong et al., 2004c; Zhong et al., 2004d). Although at first glance, it seemed intuitive that removal of FKBP52 from cells would augment AAV second-strand DNA synthesis, and consequently, transgene expression, our experimental analyses with cells derived from FKBP52-KO mice, in which FKBP52 was completely absent, documented that the transduction efficiency of AAV vectors was in fact significantly less pronounced than anticipated (Zhong et al., 2004a; Zhong et al., 2004b; Zhong et al., 2004c). Counter-intuitively, over-expression of FKBP52 led to a significant increase in the AAV transduction efficiency in a variety of murine and human established cell lines (Qing et al., 2001).

Since the level of expression of endogenous FKBP52 in semi-permissive murine NIH3T3 cells was found to be significantly lower than that in permissive human 293 cells (data not shown), we wished to determine whether FKBP52 plays an additional role in AAV-mediated transduction in primary murine cells. This was also of interest since in our previous studies, we focused our efforts on the function of FKBP52 localized in the nucleus, but FKBP52 is a cellular chaperone, and it is also localized in the cytoplasm, where it co-localizes with microtubules (Czar et al., 1994a; Czar et al., 1994b; Perrot-Applanat et al., 1995). Although the amount of FKBP52 in the cytoplasm is less than that in the nucleus, it plays crucial roles in intracellular trafficking and/or nuclear transport of a number of cellular and viral proteins, and a number of studies have focused on the function of cytoplasmic FKBP52 (Czar et al., 1994a; Czar et al., 1994b; Denny et al., 2005; Perrot-Applanat et al., 1995; Pratt, 1998; Pratt et al., 2004; Pratt, Silverstein, and Galigniana, 1999; Pratt and Toft, 1997; Wochnik et al., 2005; Wu et al., 2004).

Our previous studies have demonstrated that impaired intracellular trafficking of AAV vectors limit efficient transduction of murine cells, both established and primary, and treatment with HU increased AAV-mediated transduction efficiency in these cells by promoting nuclear transport of AAV (Hansen, Qing, and Srivastava, 2001a; Zhong et al., 2004c). Our previous studies have also documented that AAV could infect purified nuclei from human and murine cells, and in both instances, could undergo viral uncoating and second-strand DNA synthesis (Hansen, Qing, and Srivastava, 2001b). Taken together, these studies suggested that a major obstacle to efficient transduction of murine fibroblasts by AAV vectors might exist in the cytoplasm. Thus, murine fibroblasts seemed to be a suitable model to study the intracellular fate of AAV vectors.

Large particles of more than 500 Å, such as viruses and endosomes, are difficult to diffuse in the cytoplasm (Seksek, Biwersi, and Verkman, 1997). Microtubules and microfilaments not only serve as diffusion barriers but also act as “highways” to facilitate the trafficking of these particles to specific destinations such as the nucleus. Details of the intracellular pathway used by AAV are now beginning to be fully understood (Bartlett, Wilcher, and Samulski, 2000; Douar et al., 2001; Duan et al., 1999; Hansen et al., 2000; Hansen, Qing, and Srivastava,

NIH-PA Author Manuscript

NIH-PA Author Manuscript

NIH-PA Author Manuscript

2001a; Lux et al., 2005; Seisenberger et al., 2001; Warrington et al., 2004; Xiao et al., 2002). Some information is available on the relation between AAV intracellular trafficking and microtubules. For example, nocodazole-treatment to depolymerize microtubules prior to AAV infection has been shown to result in >95% reduction in the nuclear accumulation of AAV, and cytochalasin B, which disrupts microfilaments, has also been demonstrated to lead to a dramatic reduction of >90% in the nuclear accumulation of AAV (Sanlioglu et al., 2000). Trafficking on microtubules destined for either the cell center or the apical domains uses a cytoplasmic protein, dynein, since all endosome mobility ceased when dynein function was disrupted by the use of a mutant dynein heavy chain allele (Mallik and Gross, 2004; Murray and Wolkoff, 2003; Welte, 2004). Previous studies have shown that cytoplasmic dynein is less efficient and robust in achieving the comparable function to the other motors; and that it requires a number of accessory proteins as well as multiple dyneins functioning together (Welte, 2004). Information on the role of dynein in intracellular trafficking of parvoviruses is beginning to emerge (Suikkanen et al., 2002). For example, Xu *et al*., have reported that inefficient entry of AAV into NIH3T3 cells could be overcome by inserting a motif in the capsid predicted to promote binding to the LC8 subunit of the dynein motor complex (Xu et al., 2005). Additional studies have also documented that FKBP52 can bind either directly or via a linker protein with the cytoplasmic dynein; the PPIase domain fragment of FKBP52 interacts with dynein, and provides a link between the glucocorticoid receptor-HSP90 heterocomplex and cytoplasmic dynein for retrograde movement along microtubules (Galigniana et al., 2001). Unfortunately, virtually nothing is known about the role of FKBP52 on AAV intracellular trafficking. In our current studies, the association of AAV capsids with FKBP52 and dynein could be documented by co-precipitation with A20 antibodies, which specifically recognize only intact AAV particles with a defined three-dimensional structure. Although our data provide only indirect evidence for the role of FKBP52 as a nuclear chaperone for AAV in MEFs since it remains possible that the observed interaction between FKBP52, dynein, and AAV might be due to the combined effects of HU and FKBP52. However, since co-immunoprecipitation assays were carried out in 293 cells in the absence of HU in 293 cells, we believe that the observed interactions between FKBP52, dynein, and AAV are direct. Additional co-localization studies involving confocal microscopy will be needed to corroborate these observations.

AAV vectors failed to gain entry into the nucleus, and consequently failed to transduce primary murine fibroblasts. Complete removal of FKBP52 did not lead to increased transgene expression in these cells. However, FKBP52 facilitated the nuclear transport of AAV in the presence of HU in murine cells. We hypothesize that FKBP52 plays a dual role in the life cycle of AAV: the cytoplasmic FKBP52, presumably in its unphosphorylated form, helps facilitate the intracellular transport of the virus; and the nuclear FKBP52, in its phosphorylated form, strongly inhibits the viral second-strand DNA synthesis.

In sum, in addition to interacting with the D-sequence in the AAV ITR and inhibiting viral second-strand DNA synthesis, FKBP52, being a cellular chaperone protein, also facilitates intracellular trafficking of AAV. It is of interest to further explore whether the phosphorylation status of FKBP52 is a determining factor. A better understanding of the underlying molecular mechanism of intracellular trafficking of AAV should have important implications in the optimal use of recombinant AAV vectors in human gene therapy.

Materials and methods

Cells, viruses, and plasmids

Murine embryo fibroblasts (MEFs) were cultured as previously described (Horak and Flechon, 1998; Mukherjee, Guha, and Bose, 1984). In brief, 12–14 day old embryos were obtained, and a small amount of tissue was used for PCR analysis to detect the FKBP52 genotypes.

NIH-PA Author Manuscript

NIH-PA Author Manuscript

NIH-PA Author Manuscript

Fibroblasts were derived from embryos by drawing each embryo through a 10 ml syringe fitted with an 18 gauge needle. After washing, the cells were cultured in 10 cm tissue culture dishes in MEF growth media consisting of DME/F12 media (Gibco, Carlsbad, CA) containing 10% fetal bovine serum and 1% (by volume) 100×stock solution of antibiotics (10,000 U of penicillin plus 10,000 μg of streptomycin) supplemented with 2 mM L-glutamine. MEFs were immortalized at passage 3 following infection with wild-type SV40 virus at a multiplicity of infection (MOI) of 50. Immortalization had no significant effect on AAV-*lacZ* transduction efficiency (data not shown).

Highly purified stocks of a recombinant AAV2 vector containing the β-galactosidase (*lacZ*) reporter gene driven by the cytomegalovirus (CMV) immediate-early promoter (AAV2-*lacZ*) were obtained from Applied Viromics LLC, Fremont, CA. Self-complementary recombinant AAV2 vectors containing the CMV promoter-driven EGFP (scAAV2-EGFP) were generously provided by Dr. R. Jude Samulski, University of North Carolina at Chapel Hill. A recombinant expression plasmid containing the Rous sarcoma virus (RSV) promoter-driven human FKBP52 cDNA (pRSV-hFKBP52) was constructed by standard cloning methods.

Recombinant AAV2-mediated transduction assays

Approximately 8×10^4 or 3×10^5 MEFs were plated in each well in 12-well or 6-well plates, respectively, and incubated at 37°C for 12 hr. Cells were washed once with DME/F12 media and then infected at 37°C for 2 hr with mock and 5×10^3 particles per cell of recombinant AAV2-*lacZ* or scAAV2-EGFP as described previously (Qing et al., 2001; Qing et al., 1998; Qing et al., 2003; Qing et al., 1999; Qing et al., 1997). Forty-eight hours after AAV2-*lacZ* infection, cells were fixed and stained with X-gal (5-bromo-4-chloro-3-indolyl β-D-galactopyranoside) and the blue cells were counted, or β-galactosidase activity was measured by Galacto-Light Plus chemiluminiscence reporter assay (Applied Biosystems, Foster City, CA) according to the manufacturer's instructions. Data were expressed as relative light units (RLU) per microgram of total protein and were within the linear range of the assay. The transduction efficiency of scAAV2-EGFP was measured by GFP imaging using a Zeiss Axiovert 25 fluorescence microscope (Carl Zeiss, Inc., Thornwood, NY). Images from three visual fields of mock-infected and vector-infected MEFs cells 48 h post-injection were analyzed quantitatively by ImageJ analysis software (NIH, Bethesda, MD). Transgene expression was assessed as total area of green fluorescence ($pixel^2$) per visual field (mean±SD).

Preparation of whole cell extracts (WCEs) and electrophoretic mobility-shift assays (EMSA)

WCEs from MEFs were prepared according to the method of Muller (Muller, 1987). Total protein concentration was determined by the Bio-Rad protein assay kit (Bio-Rad, Hercules, CA), and the extracts were frozen in liquid N_2 and stored at −70°C. EMSA were performed as described previously (Qing et al., 2001; Qing et al., 1998; Qing et al., 2003; Qing et al., 1997; Zhong et al., 2004d). Briefly, DNA-binding reactions were performed in a volume of 20 μl with 2 μg of poly (dI-dC), 2 μg of bovine serum albumin, and 12% glycerol in Tris buffer (10 mM Tris-HCl, 0.5 mM dithiothreitol, 25 mM NaCl, 5 mM $MgCl_2$, 0.05% Nonidet P-40 [NP40], pH 8.0). Ten μg of protein of each WCEs were pre-incubated for 10 min at 25°C followed by the addition of 10,000 cpm of ^{32}P-labeled D-sequence synthetic oligonucleotide (5′-AGGAACCCCTAGTGATGGAG-3′) in the reaction mixture. The binding reaction was allowed to proceed for 30 min at 25°C. Bound complexes were separated from the free probe on low ionic strength 4% polyacrylamide gels with Tris-glycine/EDTA buffer, pH 8.5, containing 50 mM Tris-HCl, 380 mM glycine, and 2 mM EDTA. Following electrophoresis, the gel was dried in vacuum and autoradiographed using Kodak X-Omat film at −70°C.

NIH-PA Author Manuscript

NIH-PA Author Manuscript

NIH-PA Author Manuscript

Southern blot analyses for AAV internalization

Approximately 3×10^6 MEFs from each genotype were either mock-infected or infected with 3×10^3 particles/cell of AAV2-*lacZ* for 2 hr at 37°C after which cells were treated with 0.01% trypsin and washed extensively with PBS to remove any adsorbed and unadsorbed virus particles. Low M_r DNA was isolated and electrophoresed on 1% agarose gels followed by Southern blot hybridization with a ^{32}P-labeled *lacZ*-specific DNA probe as described previously (Hansen et al., 2000; Hansen, Qing, and Srivastava, 2001a).

Isolation of nuclear and cytoplasmic fractions from MEFs and Southern blot analyses for AAV intracellular trafficking

Nuclear and cytoplasmic fractions from MEFs were isolated as described previously (Hansen et al., 2000; Hansen, Qing, and Srivastava, 2001a; Zhong et al., 2004c). Briefly, MEFs mock infected or infected with the recombinant AAV-*lacZ* vectors were washed twice with PBS. The cell pellets were gently resuspended in 200 µl of homogenization buffer (0.25 M sucrose, 10 mM triethanolamine, pH 7.6, 1 mM EDTA, 0.1 mM phenylmethylsulfonyl fluoride [PMSF]) and incubated on ice for 5 min, after which 10 µl of 10% NP-40 was added to each tube and cells were observed under a light microscope for about 2 min. The samples were then mixed gently and centrifuged for 5 min at 500 rpm at 4°C. The supernatants (cytoplasmic fraction) were decanted and stored on ice. The pellets (nuclear fractions) were washed twice with 1 ml of homogenization buffer and stored on ice. The purity of each fraction was determined to be >95%, as measured by the absence of acid phosphatase activity (nuclear fractions) and the absence of histone H3 (cytoplasmic fractions) as described previously (Hansen et al., 2000; Hansen, Qing, and Srivastava, 2001a; Zhong et al., 2004c). Low M_r DNA samples from nuclear and cytoplasmic fractions were isolated and electrophoresed on 1% agarose gels followed by Southern blot as described above. Densitometric scanning of autoradiographs, for the quantitation of relative amounts of viral genomes, was evaluated with ImageJ analysis software.

Stable transfection with FKBP52 expression plasmids

Approximately 4×10^5 MEFs from FKBP52-KO mice were seeded into each well in a 6-well plate in DME/F12 media (Gibco, Carlsbad, CA) containing 10% fetal bovine serum for 24 h prior to transfection. Four µg of pRSV-FKBP52 was added to cells using Lipofectamine™ 2000 Reagent (Invitrogen, Carlsbad, CA) according to the manufacturer's instructions. Cells were cultured in the selective media containing 300 mg/ml hygromycin (Invitrogen) 48 hours after transfection. Clones containing FKBP52 vectors were obtained after 28 days of selection.

Immunoprecipitations and Western blot analyses

To determine the levels of FKBP52 in MEFs from FKBP52-WT, HE and KO mice, and in MEFs from FKBP52-KO mice stably transfected with FKBP52 expression plasmid, approximately 3×10^6 cells were seeded in culture dishes, and 24 h later, WCEs were prepared. Total protein concentrations were determined using the Bio-Rad protein assay kit, and 40µg of protein was separated by SDS-polyacrylamide gel electrophoresis on a 10% polyacrylamide gel. After transfer to an Immobilon-P membrane (Millipore, Bedford, MA), the membrane was blocked at 25°C for 1 h with 5% nonfat dry milk in 1× Tris-buffered saline (TBS; 20 mM Tris-HCl, pH 7.5, 150 mM NaCl), and 0.05% Tween 20, then incubated with a 1:500 dilution of anti-FKBP52 antibody for 1 h at 25°C. Following incubation with 1:5,000 dilution of horseradish peroxidase-coupled anti-rabbit IgG antibody for at 25°C 1 h and protein bands were visualized with the ECL-Plus chemiluminiscence detection kit (Amersham Biosciences, Piscataway, NJ) according to the instructions provided by the manufacturer.

NIH-PA Author Manuscript

NIH-PA Author Manuscript

NIH-PA Author Manuscript

For immunoprecipitation, five 150 mm plates 293 cells were triple transfected by pAAV-hrGFP, pHelper and pAAV2-RC to produce AAV vector with lipofectamine, and the cells were harvested at 72 h post-transfection by scraping and resuspended in 2ml hypotonic buffer (20 mM HEPES pH 7.5, 5 mM KCl, 0.5 mM $MgCl_2$, 1 mM DTT, 0.1 mM PMSF, 2 mM pepstatin A), and the cytoplasm was isolated by homogenization in a tight-fitting Duall tissue grinder until about 80% cell lysis was achieved as monitored by trypan blue. Equivalent amounts of cytoplasm were cleared of nonspecific binding by incubation with 0.25 mg of normal goat IgG together with 20 μl of protein G-agarose beads for 60 min at 4°C in an orbital shaker. After pre-clearing, 2 μg of A20 antibody (mouse IgG) or 2 μg of normal mouse IgG (as a negative control) were added and incubated at 4°C for 1 h, followed by precipitation with protein G-agarose beads at 4°C for 12 h in the shaker. Pellets were collected by centrifugation at 2,500 rpm for 5 min at 4°C and washed four times with phosphate-buffered saline. After the final wash, the supernatant was aspirated and discarded, and the pellet was resuspended in equal volume of 2x SDS sample buffer. Twenty μl of resuspended pellet solutions were used for Western blotting with anti-B1, anti-FKBP52 and anti-dynein intermediate chain antibodies (Sigma, USA).

Acknowledgments

We thank Dr. Jacqueline A. Hobbs for a critical review of this manuscript, and Ms. Irene Zolotukhin for her expert technical assistance. This work was supported in part by United States Public Health Service Grants R01 EB-002073, R01 HL-65570, and R01 HL-76901 from the National Institutes of Health (to AS).

References

Bartlett JS, Wilcher R, Samulski RJ. Infectious entry pathway of adeno-associated virus and adeno-associated virus vectors. J Virol 2000;74(6):2777–2785. [PubMed: 10684294]

Berns KI, Giraud C. Biology of adeno-associated virus. Curr Top Microbiol Immunol 1996;218:1–23. [PubMed: 8794242]

Conlon TJ, Flotte TR. Recombinant adeno-associated virus vectors for gene therapy. Expert Opin Biol Ther 2004;4(7):1093–1101. [PubMed: 15268676]

Czar MJ, Owens-Grillo JK, Dittmar KD, Hutchison KA, Zacharek AM, Leach KL, Deibel MR Jr, Pratt WB. Characterization of the protein-protein interactions determining the heat shock protein (hsp90.hsp70.hsp56) heterocomplex. J Biol Chem 1994a;269(15):11155–11161. [PubMed: 8157642]

Czar MJ, Owens-Grillo JK, Yem AW, Leach KL, Deibel MR Jr, Welsh MJ, Pratt WB. The hsp56 immunophilin component of untransformed steroid receptor complexes is localized both to microtubules in the cytoplasm and to the same nonrandom regions within the nucleus as the steroid receptor. Mol Endocrinol 1994b;8(12):1731–1741. [PubMed: 7708060]

Denny WB, Prapapanich V, Smith DF, Scammell JG. Structure-function analysis of squirrel monkey FK506-binding protein 51, a potent inhibitor of glucocorticoid receptor activity. Endocrinology 2005;146(7):3194–3201. [PubMed: 15802496]

Douar AM, Poulard K, Stockholm D, Danos O. Intracellular trafficking of adeno-associated virus vectors: routing to the late endosomal compartment and proteasome degradation. J Virol 2001;75(4):1824–1833. [PubMed: 11160681]

Duan D, Li Q, Kao AW, Yue Y, Pessin JE, Engelhardt JF. Dynamin is required for recombinant adeno-associated virus type 2 infection. J Virol 1999;73(12):10371–10376. [PubMed: 10559355]

Ferrari FK, Samulski T, Shenk T, Samulski RJ. Second-strand synthesis is a rate-limiting step for efficient transduction by recombinant adeno-associated virus vectors. J Virol 1996;70(5):3227–3234. [PubMed: 8627803]

Fisher KJ, Gao GP, Weitzman MD, DeMatteo R, Burda JF, Wilson JM. Transduction with recombinant adeno-associated virus for gene therapy is limited by leading-strand synthesis. J Virol 1996;70(1):520–532. [PubMed: 8523565]

Galigniana MD, Radanyi C, Renoir JM, Housley PR, Pratt WB. Evidence that the peptidylprolyl isomerase domain of the hsp90-binding immunophilin FKBP52 is involved in both dynein interaction

NIH-PA Author Manuscript

NIH-PA Author Manuscript

NIH-PA Author Manuscript

and glucocorticoid receptor movement to the nucleus. J Biol Chem 2001;276(18):14884–14889. [PubMed: 11278753]

Hansen J, Qing K, Kwon HJ, Mah C, Srivastava A. Impaired intracellular trafficking of adeno-associated virus type 2 vectors limits efficient transduction of murine fibroblasts. J Virol 2000;74(2):992–996. [PubMed: 10623762]

Hansen J, Qing K, Srivastava A. Adeno-associated virus type 2-mediated gene transfer: altered endocytic processing enhances transduction efficiency in murine fibroblasts. J Virol 2001a;75(9):4080–4090. [PubMed: 11287557]

Hansen J, Qing K, Srivastava A. Infection of purified nuclei by adeno-associated virus 2. Mol Ther 2001b; 4(4):289–296. [PubMed: 11592830]

Horak V, Flechon JE. Immunocytochemical characterisation of rabbit and mouse embryonic fibroblasts. Reprod Nutr Dev 1998;38(6):683–695. [PubMed: 9932301]

Lux K, Goerlitz N, Schlemminger S, Perabo L, Goldnau D, Endell J, Leike K, Kofler D, Finke S, Hallek M, Buning H. Green fluorescent protein-tagged adeno-associated virus particles allow the study of cytosolic and nuclear trafficking. J Virol 2005;79(18):11776–11787. [PubMed: 16140755]

Mah C, Qing K, Khuntirat B, Ponnazhagan S, Wang XS, Kube DM, Yoder MC, Srivastava A. Adeno-associated virus type 2-mediated gene transfer: role of epidermal growth factor receptor protein tyrosine kinase in transgene expression. J Virol 1998;72(12):9835–9843. [PubMed: 9811719]

Mallik R, Gross SP. Molecular motors: strategies to get along. Curr Biol 2004;14(22):R971–R982. [PubMed: 15556858]

Marshall E. Gene therapy. Viral vectors still pack surprises. Science 2001;294(5547):1640. [PubMed: 11721031]

McCarty DM, Monahan PE, Samulski RJ. Self-complementary recombinant adeno-associated virus (scAAV) vectors promote efficient transduction independently of DNA synthesis. Gene Ther 2001;8 (16):1248–1254. [PubMed: 11509958]

Mukherjee P, Guha S, Bose SR. Chemical transformation of Swiss mouse embryo fibroblasts in primary culture. Neoplasma 1984;31(5):557–564. [PubMed: 6504214]

Muller MT. Binding of the herpes simplex virus immediate-early gene productCP4 to its own transcription start site. J Virol 1987;61(3):858–865. [PubMed: 3027412]

Murray JW, Wolkoff AW. Roles of the cytoskeleton and motor proteins in endocytic sorting. Adv Drug Deliv Rev 1992;55(11):1385–1403. [PubMed: 14597137]

Muzyczka N. Use of adeno-associated virus as a general transduction vector for mammalian cells. Curr Top Microbiol Immunol 1992;158:97–129. [PubMed: 1316261]

Perrot-Applanat M, Cibert C, Geraud G, Renoir JM, Baulieu EE. The 59 kDa FK506-binding protein, a 90 kDa heat shock protein binding immunophilin (FKBP59-HBI), is associated with the nucleus, the cytoskeleton and mitotic apparatus. J Cell Sci 1995;108(Pt 5):2037–2051. [PubMed: 7544801]

Pratt WB. The hsp90-based chaperone system: involvement in signal transduction from a variety of hormone and growth factor receptors. Proc Soc Exp Biol Med 1998;217(4):420–434. [PubMed: 9521088]

Pratt WB, Galigniana MD, Harrell JM, DeFranco DB. Role of hsp90 and the hsp90-binding immunophilins in signalling protein movement. Cell Signal 2004;16(8):857–872. [PubMed: 15157665]

Pratt WB, Silverstein AM, Galigniana MD. A model for the cytoplasmic trafficking of signalling proteins involving the hsp90-binding immunophilins and p50cdc37. Cell Signal 1999;11(12):839–851. [PubMed: 10659992]

Pratt WB, Toft DO. Steroid receptor interactions with heat shock protein and immunophilin chaperones. Endocr Rev 1997;18(3):306–360. [PubMed: 9183567]

Qing K, Hansen J, Weigel-Kelley KA, Tan M, Zhou S, Srivastava A. Adeno-associated virus type 2-mediated gene transfer: role of cellular FKBP52 protein in transgene expression. J Virol 2001;75 (19):8968–8976. [PubMed: 11533160]

Qing K, Khuntirat B, Mah C, Kube DM, Wang XS, Ponnazhagan S, Zhou S, Dwarki VJ, Yoder MC, Srivastava A. Adeno-associated virus type 2-mediated gene transfer: correlation of tyrosine phosphorylation of the cellular single-stranded D sequence-binding protein with transgene expression in human cells in vitro and murine tissues in vivo. J Virol 1998;72(2):1593–1599. [PubMed: 9445062]

NIH-PA Author Manuscript

NIH-PA Author Manuscript

NIH-PA Author Manuscript

Qing K, Li W, Zhong L, Tan M, Hansen J, Weigel-Kelley KA, Chen L, Yoder MC, Srivastava A. Adeno-associated virus type 2-mediated gene transfer: role of cellular T-cell protein tyrosine phosphatase in transgene expression in established cell lines in vitro and transgenic mice in vivo. J Virol 2003;77 (4):2741–2746. [PubMed: 12552015]

Qing K, Mah C, Hansen J, Zhou S, Dwarki V, Srivastava A. Human fibroblast growth factor receptor 1 is a co-receptor for infection by adeno-associated virus 2. Nat Med 1999;5(1):71–77. [PubMed: 9883842]

Qing K, Wang XS, Kube DM, Ponnazhagan S, Bajpai A, Srivastava A. Role of tyrosine phosphorylation of a cellular protein in adeno-associated virus 2-mediated transgene expression. Proc Natl Acad Sci U S A 1997;94(20):10879–10884. [PubMed: 9380728]

Russell DW, Alexander IE, Miller AD. DNA synthesis and topoisomerase inhibitors increase transduction by adeno-associated virus vectors. Proc Natl Acad Sci U S A 1995;92(12):5719–5723. [PubMed: 7777575]

Sanchez ER, Faber LE, Henzel WJ, Pratt WB. The 56–59-kilodalton protein identified in untransformed steroid receptor complexes is a unique protein that exists in cytosol in a complex with both the 70- and 90-kilodalton heat shock proteins. Biochemistry 1990;29(21):5145–5152. [PubMed: 2378870]

Sanlioglu S, Benson PK, Yang J, Atkinson EM, Reynolds T, Engelhardt JF. Endocytosis and nuclear trafficking of adeno-associated virus type 2 are controlled by rac1 and phosphatidylinositol-3 kinase activation. J Virol 2000;74(19):9184–9196. [PubMed: 10982365]

Schmitt J, Pohl J, Stunnenberg HG. Cloning and expression of a mouse cDNA encoding p59, an immunophilin that associates with the glucocorticoid receptor. Gene 1993;132(2):267–271. [PubMed: 7693550]

Seisenberger G, Ried MU, Endress T, Buning H, Hallek M, Brauchle C. Real-time single-molecule imaging of the infection pathway of an adeno-associated virus. Science 2001;294(5548):1929–1932. [PubMed: 11729319]

Seksek O, Biwersi J, Verkman AS. Translational diffusion of macromolecule-sized solutes in cytoplasm and nucleus. J Cell Biol 1997;138(1):131–142. [PubMed: 9214387]

Suikkanen S, Saajarvi K, Hirsimaki J, Valilehto O, Reunanen H, Vihinen-Ranta M, Vuento M. Role of recycling endosomes and lysosomes in dynein-dependent entry of canine parvovirus. J Virol 2002;76 (9):4401–4411. [PubMed: 11932407]

Summerford C, Bartlett JS, Samulski RJ. AlphaVbeta5 integrin: a co-receptor for adeno-associated virus type 2 infection. Nat Med 1999;5(1):78–82. [PubMed: 9883843]

Wang Z, Ma HI, Li J, Sun L, Zhang J, Xiao X. Rapid and highly efficient transduction by double-stranded adeno-associated virus vectors in vitro and in vivo. Gene Ther 2003;10(26):2105–2111. [PubMed: 14625564]

Warrington KH Jr, Gorbatyuk OS, Harrison JK, Opie SR, Zolotukhin S, Muzyczka N. Adeno-associated virus type 2 VP2 capsid protein is nonessential and can tolerate large peptide insertions at its N terminus. J Virol 2004;78(12):6595–6609. [PubMed: 15163751]

Welte MA. Bidirectional transport along microtubules. Curr Biol 2004;14(13):R525–R537. [PubMed: 15242636]

Wistuba A, Kern A, Weger S, Grimm D, Kleinschmidt JA. Subcellular compartmentalization of adeno-associated virus type 2 assembly. J Virol 1997;71(2):1341–1352. [PubMed: 8995658]

Wobus CE, Hugle-Dorr B, Girod A, Petersen G, Hallek M, Kleinschmidt JA. Monoclonal antibodies against the adeno-associated virus type 2 (AAV-2) capsid: epitope mapping and identification of capsid domains involved in AAV-2-cell interaction and neutralization of AAV-2 infection. J Virol 2000;74(19):9281–9293. [PubMed: 10982375]

Wochnik GM, Ruegg J, Abel GA, Schmidt U, Holsboer F, Rein T. FK506-binding proteins 51 and 52 differentially regulate dynein interaction and nuclear translocation of the glucocorticoid receptor in mammalian cells. J Biol Chem 2005;280(6):4609–4616. [PubMed: 15591061]

Wu B, Li P, Liu Y, Lou Z, Ding Y, Shu C, Ye S, Bartlam M, Shen B, Rao Z. 3D structure of human FK506-binding protein 52: implications for the assembly of the glucocorticoid receptor/Hsp90/ immunophilin heterocomplex. Proc Natl Acad Sci U S A 2004;101(22):8348–8353. [PubMed: 15159550]

NIH-PA Author Manuscript

NIH-PA Author Manuscript

NIH-PA Author Manuscript

Xiao W, Warrington KH Jr, Hearing P, Hughes J, Muzyczka N. Adenovirus-facilitated nuclear translocation of adeno-associated virus type 2. J Virol 2002;76(22):11505–11517. [PubMed: 12388712]

Xu J, Ma C, Bass C, Terwilliger EF. A combination of mutations enhances the neurotropism of AAV-2. Virology 2005;341(2):203–214. [PubMed: 16102794]

Zhong L, Chen L, Li Y, Qing K, Weigel-Kelley KA, Chan RJ, Yoder MC, Srivastava A. Self-complementary adeno-associated virus 2 (AAV)-T cell protein tyrosine phosphatase vectors as helper viruses to improve transduction efficiency of conventional single-stranded AAV vectors in vitro and in vivo. Mol Ther 2004a;10(5):950–957. [PubMed: 15509512]

Zhong L, Li W, Yang Z, Chen L, Li Y, Qing K, Weigel-Kelley KA, Yoder MC, Shou W, Srivastava A. Improved transduction of primary murine hepatocytes by recombinant adeno-associated virus 2 vectors in vivo. Gene Ther 2004b;11(14):1165–1169. [PubMed: 15164097]

Zhong L, Li W, Yang Z, Qing K, Tan M, Hansen J, Li Y, Chen L, Chan RJ, Bischof D, Maina N, Weigel-Kelley KA, Zhao W, Larsen SH, Yoder MC, Shou W, Srivastava A. Impaired nuclear transport and uncoating limit recombinant adeno-associated virus 2 vector-mediated transduction of primary murine hematopoietic cells. Hum Gene Ther 2004c;15(12):1207–1218. [PubMed: 15684697]

Zhong L, Qing K, Si Y, Chen L, Tan M, Srivastava A. Heat-shock treatment-mediated increase in transduction by recombinant adeno-associated virus 2 vectors is independent of the cellular heat-shock protein 90. J Biol Chem 2004d;279(13):12714–12723. [PubMed: 14711833]

NIH-PA Author Manuscript

NIH-PA Author Manuscript

NIH-PA Author Manuscript

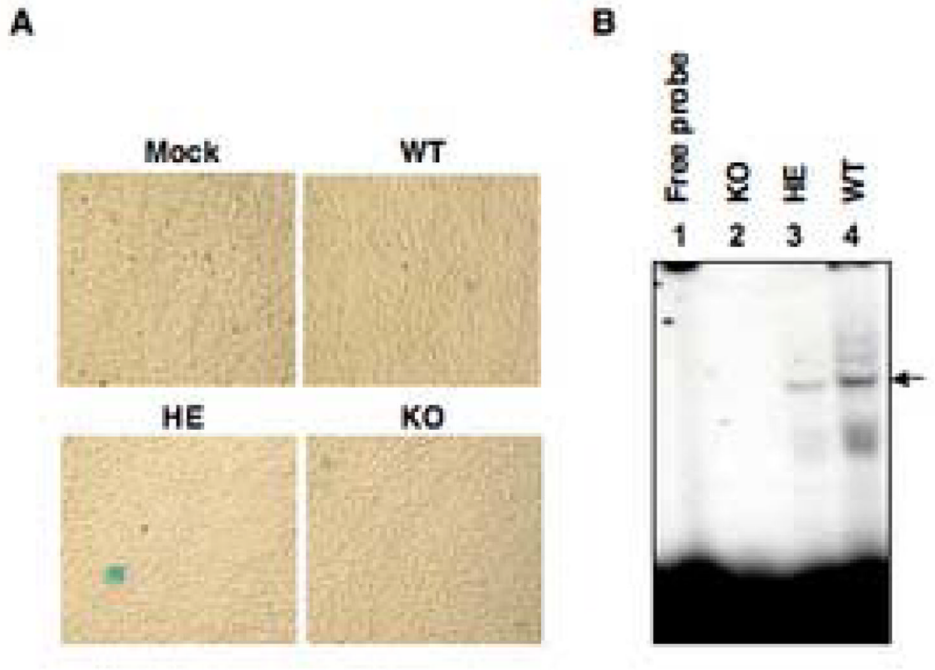

FIG. 1.

A. Comparative analyses of AAV-mediated transduction efficiency in MEFs from FKBP52-WT, HE and KO mice. Approximately 3×10^5 MEFs were plated in each well in a 6-well plate. Cells were either mock-infected or infected with 5×10^3 particles/cell of AAV2-*lacZ* in identical conditions. Cells were fixed, stained with X-gal 48 h post-infection, and photographed using a Nikon inverted light microscope. Original magnification, 100×. **B.** Electrophoretic mobility shift assays for interaction between AAV D-sequence and WCEs of MEFs from three FKBP52 genotypes mice. The radiolabeled AAV D-sequence probe (lane 1) forms a complex when incubated with WCEs of MEFs from FKBP52-WT mice (lane 4), but does not interact with those from FKBP52-KO mice (lane 2), and the interaction with that from FKBP52-HE mice is reduced by ~50% (lane 3). Complex of FKBP52 and D-sequence probe is denoted by the arrow.

NIH-PA Author Manuscript

NIH-PA Author Manuscript

NIH-PA Author Manuscript

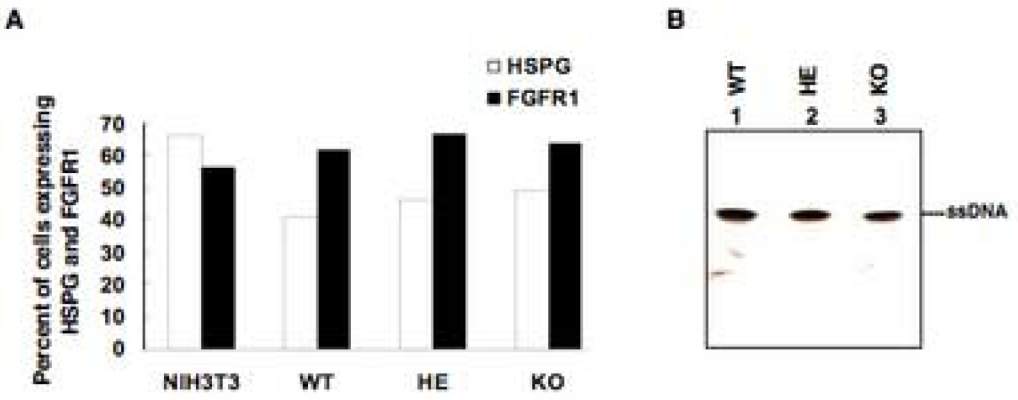

FIG. 2.

A. Comparative analyses of the levels of cell surface expression of heparan sulfate proteoglycan (HSPG) and fibroblast growth factor receptor 1 (FGFR1) in NIH3T3 cells and MEFs from FKBP52-WT, HE and KO mice by fluorescence-activated cell sorting (FACS). **B.** Southern blot analyses of the AAV-*lacZ* DNA entry into MEFs from FKBP52-KO, HE, and WT mice. MEFs from each genotype were infected with 3×10^3 particles/cell of AAV2-*lacZ* for 2 hr at 37°C. Low M_r DNA was isolated and analyzed by Southern blot hybridization using a ^{32}P-labeled *lacZ*-specific DNA probe. ssDNA denotes the viral single-stranded DNA genomes.

NIH-PA Author Manuscript

NIH-PA Author Manuscript

NIH-PA Author Manuscript

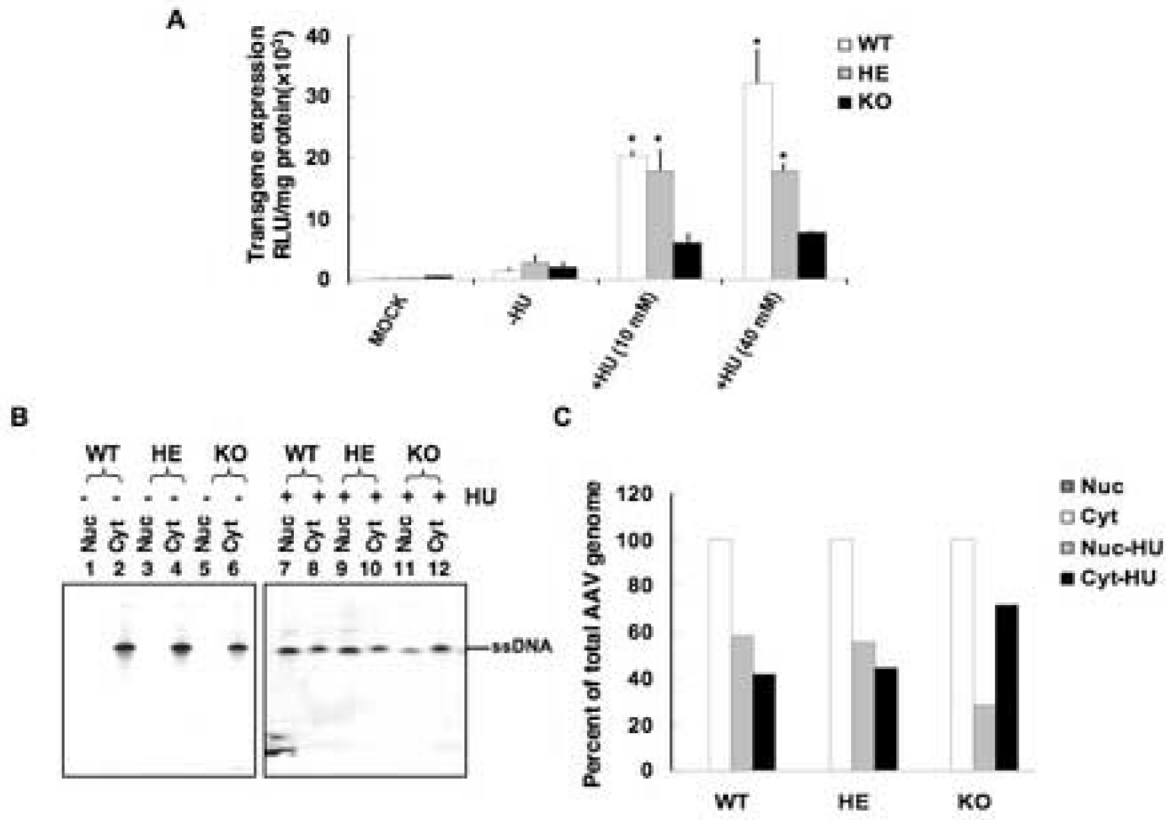

FIG. 3.

A. Comparative analyses of the effect of HU treatment on the transduction efficiency of single-stranded, conventional AAV vectors in MEFs from FKBP52-WT, HE and KO mice. Cells were mock-treated or treated with 40 mM HU and either mock infected or infected with 5×10^3 particles/cell of conventional, single-stranded recombinant AAV-*lacZ* vectors. Forty-eight hours post-infection, β-galactosidase activity was measured by Galacto-Light Plus chemiluminiscence reporter assay according to the manufacturer's instructions. **B**. Southern blot analyses of cytoplasmic and nuclear distribution of AAV-*lacZ* genomes in MEFs from FKBP52 WT, HE and KO mice without (Lanes 1–6) and with (Lanes 7–12) HU treatment. MEFs from each genotype were infected with ~1×10^4 particles/cell of AAV2-*lacZ* for 48 h at 37°C. Low M_r DNA was isolated and analyzed by Southern blot hybridization using a ^{32}P-labeled *lacZ*-specific DNA probe. ssDNA denotes the viral single-stranded DNA genomes. **C.** Quantitative analyses of cytoplasmic and nuclear distribution of AAV-*lacZ* genomes in MEFs from FKBP52 WT, HE and KO mice, with and without HU- treatment. **p*<0.001 *versus* control and KO-MEFs.

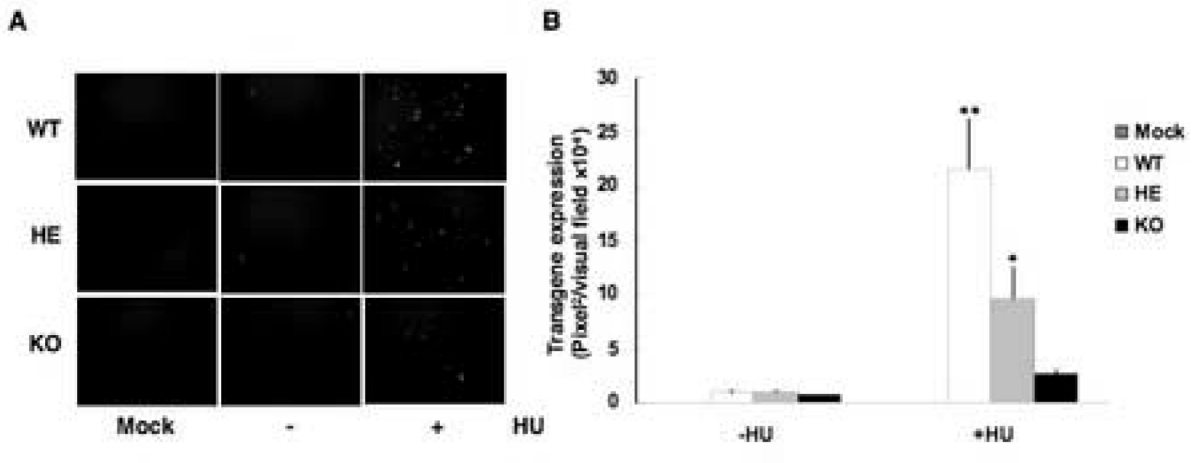

FIG. 4.

A. Comparative analyses of the effect of HU treatment on the transduction efficiency of double-stranded, self-complementary AAV vectors in MEFs from FKBP52-WT, HE and KO mice. Cells were mock-treated or treated with 40mM HU and either mock infected or infected with 5×10^3 particles/cell of recombinant scAAV-EGFP vectors. Transgene expression was detected by fluorescence microscopy 48 h post-infection. Original magnification 100×. **B.** Quantitative analyses of scAAV transduction efficiency. Images from three visual fields were analyzed quantitatively by ImageJ analysis software. Transgene expression was assessed as total area of green fluorescence (pixel^2) per visual field (mean±SD). *p<0.001, *versus* control, and p<0.01 *versus* KO MEFs, **p<0.001 *versus* control and KO MEFs.

NIH-PA Author Manuscript NIH-PA Author Manuscript NIH-PA Author Manuscript

NIH-PA Author Manuscript

NIH-PA Author Manuscript

NIH-PA Author Manuscript

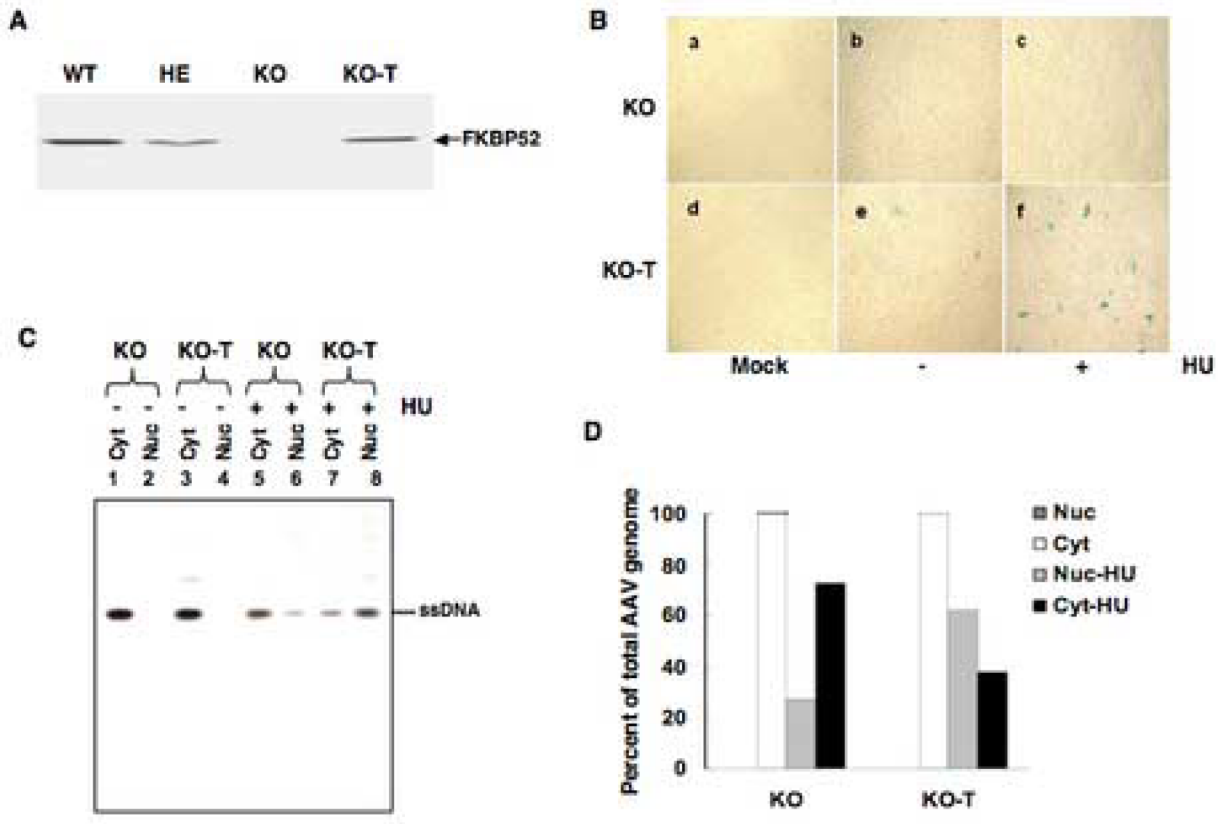

FIG. 5.

A. Western blot analysis for the expression of FKBP52 in MEFs from FKBP52 WT, HE and KO mice, and in KO cells stably transfected with an FKBP52 expression plasmid (KO-T). **B.** Comparative analyses of AAV-mediated transduction efficiency in KO and KO-T cells. Cells were either mock infected or infected with 5×10^3 particles/cell recombinant AAV-*lacZ* vectors under identical conditions. **C.** Southern blot analyses of cytoplasmic and nuclear distribution of AAV-*lacZ* genomes in KO and KO-T cells, with and without HU treatment. **D.** Quantitative analyses of the data in Panel **C**.

NIH-PA Author Manuscript

NIH-PA Author Manuscript

NIH-PA Author Manuscript

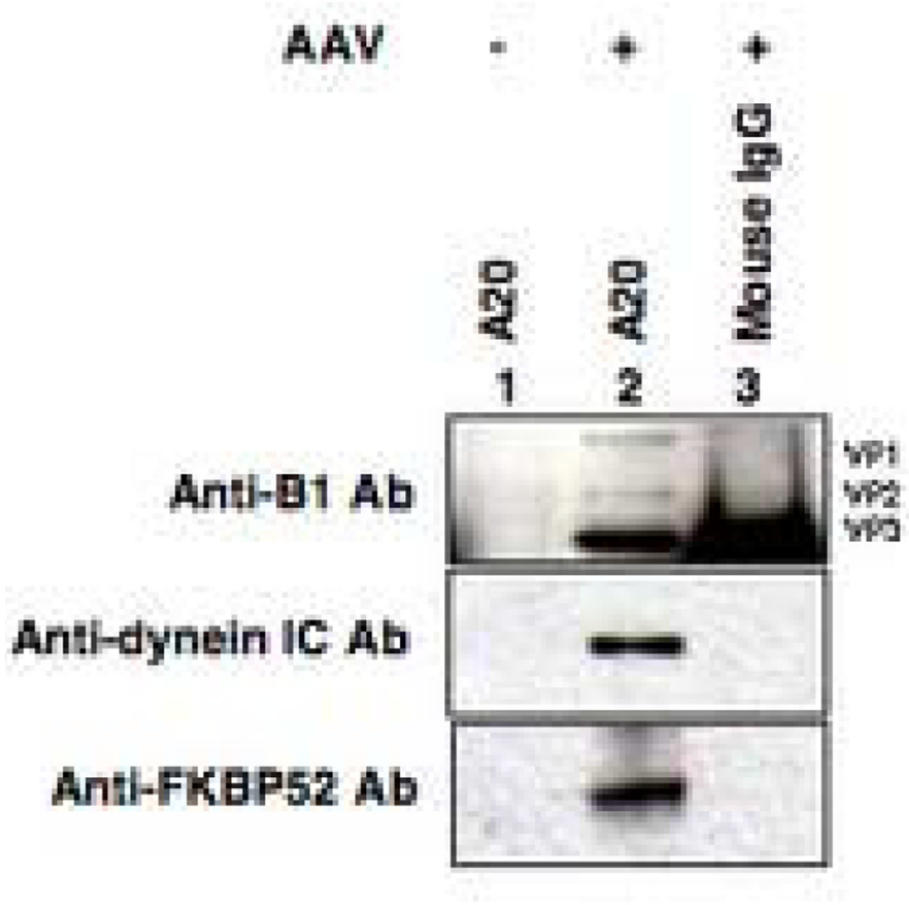

FIG. 6.

Western blot analyses for interaction of AAV capsids with FKBP52. 293 cells were mock-transfected (lane 1) or triple-transfected with pAAV-hrGFP, pHelper, and pAAV2-RC plasmids (lanes 2 and 3) to generate recombinant AAV-GFP vectors. Cells were harvested 72 h post-transfection, cytoplasmic fractions isolated, and immunoprecipitated with A20 antibodies (lanes 1 and 2), or normal mouse IgG (lane 3), and probed with anti-B1 AAV antibodies (top panel), anti-dynein intermediate chain (IC) antibodies (middle panel), and anti-FKBP52 antibodies (bottom panel).